Thresholds for Several Photo-Nuclear Reactions

J. McElhinney,* A. O. Hanson, R. A. Becker, R. B. Duffield, and B. C. Diven
Physics Research Laboratory, University of Illinois, Champaign, Illinois

(Received November 1, 1948)

The x-rays from a 22-Mev betatron were used to observe the thresholds for 23 photo-nuclear reactions which are listed in Table I. The observed thresholds are compared with the mass data for the lighter elements and with those obtained from an empirical treatment of the masses for the heavier elements.

The excitation curves were extended up to 21 Mev in a few cases. These curves were very much alike except that for the Ta(γ, n) reaction. This curve showed an abrupt decrease in slope at about 18 Mev which indicates a much reduced cross section for photons above this energy.

INTRODUCTION

THE use of the 22-Mev betatron for the production of x-rays with an accurately controlled maximum energy has been described by Baldwin and Koch. Data on the excitation functions near thresholds were presented for photo-neutron reactions in N, C, O, Fe, Cu, Zn, Mo, and Ag.[1]

The present report describes additional work with a number of other elements. The preliminary results have already been reported briefly.[2] The experimental arrangement was essentially the same as that of the earlier work but the development of the betatron during the past few years has made the x-ray intensity available about 20 times greater. It was, therefore, profitable to repeat some of the previous work, in particular that on the light elements which serve to establish the energy scale.

Determination of X-Ray Energy

The energy of the electrons as they strike the x-ray target is controlled as in the previous work by the voltage across a condenser which is placed in series with a large resistance across one of the betatron coils. The voltage across this condenser is proportional to the integral of the applied voltage and to the magnetic field at the orbit. Since the radius of the target is fixed, the momentum of the electrons is proportional to the voltage across the condenser. The kinetic energy of the electron can be determined by adjusting the bias on a trigger circuit so that the orbit expander is fired at a predetermined value of this condenser voltage. The kinetic energy of the electrons or maximum x-ray energy can then be expressed in terms of the integrator bias by means of the relation,

$$T=[K(I-I_0)/\beta]-0.51 \text{ Mev}, \qquad (1)$$

where K is an empirically determined constant, I the integrator bias voltage; I_0 the zero error caused by contact potentials and other biases in the trigger circuit. β is the ratio of the velocity of the electron to that of light and can be taken as unity for all but the lowest energies used in this work.

The determination of the electron and x-ray energies by the simple considerations mentioned above is not quite accurate since the energy is changed by the additional flux introduced by the expander. If the electron orbit during acceleration is fixed, this additional pulse should be strictly proportional to the initial magnetic field at the time of the expansion and would not introduce any non-linear corrections in the energy scale. Estimates of the non-linear corrections resulting from this effect are of the order of 0.02 Mev and were neglected since these corrections are small compared to the uncertainties in determining actual threshold energies.

Another source of non-linearity in the energy scale based on the integrator bias may be introduced by a constant time delay between the firing of the trigger circuit and the firing of the expander circuit. These time delays were accurately measured and were taken into account

* Now at Los Alamos Scientific Laboratory, Los Alamos, New Mexico.

[1] G. C. Baldwin and H. W. Koch, Phys. Rev. **67**, 1 (1945); Phys. Rev. **63**, 462A (1943).

[2] R. A. Becker, A. O. Hanson, and B. C. Diven, Phys. Rev. **71**, 466A (1947); J. McElhinney, A. O. Hanson and R. B. Duffield, Bull. Am. Phys. Soc. **23**, 4 (1948).

in the estimated errors made in the process of expansion. There is, however, a similar error which could be introduced by a slight shift in phase between the effective integrator signal and the actual magnetic field in the betatron. Any significant error of this type can be detected by a change in the integrator bias voltage corresponding to a fixed nuclear threshold, such as that of copper, upon changing the amplitude of the exciting current in the main coils of the magnet. Actual tests for this type of error were not conclusive. Individual runs indicated changes in the bias settings for copper of from 0 to 0.3 percent.

Since the non-linear corrections were small and somewhat uncertain, it was thought that the most reliable energy scale could be obtained by using known fixed points to establish a linear relation between the integrator bias and the maximum x-ray energy. The fixed points examined for this purpose were the thresholds of beryllium and deuterium at low energies and that of carbon and nitrogen at the higher energies. The thresholds of beryllium and carbon could be quite accurately defined and served to establish the energy scale used in this work. This scale places the threshold for Cu^{63} at 10.9 ± 0.2 Mev which is the same as that used by Baldwin and Koch. A recent magnetic field measurement gave a value of 11.0 ± 0.2 Mev. A direct comparison of this copper threshold with that of N^{14} indicated a value of about 10.76 ± 0.2 Mev if the nitrogen threshold is taken as 10.51 Mev. The scale chosen seems to be a fair compromise between the various data and should serve until more reliable absolute values of some of these thresholds become available.

Experimental Arrangements

Since the method of observation of the excitation curves for various reactions depends on the nature of the induced activity, it is necessary to describe the results in each case individually. The data presented here were not all obtained at the same time, but were grouped in the following way.

1. Short period activities in Li, Mg, Al, Si, S, and Ca were detected by irradiating cylindrical samples at the monitor position shown in Fig. 1 and allowing them to drop over a Geiger counter at the end of a short irradiation. The scaled counts were recorded as a function of time by means of an Esterline Angus recording milliammeter. The analysis of the record provided a reliable measure of the amount of the short period activity present. This will be referred to as the drop method. These data do not give very sensitive measurements of the thresholds for the activities because of the low yields and the short counting times involved.

2. Long period activities and complete excitation curves for Mg, Cu, and Ta involved irradiations of the order of one hour. The induced radioactivity was again recorded on the recording milliammeters. With two recorders equipped with side pens it was possible to record the output of six counters simultaneously. The data for the individual activities were then taken from these records.

3. The use of rhodium neutron detectors to determine thresholds by the observation of neutrons from the reaction was first used in the case of bismuth, which gave no measurable radioactivity but was found to have a well-defined threshold for the emission of neutrons. This method was later used in the observation of the thresholds of beryllium, deuterium, and iodine.

4. The last set of measurements was made to check the energy scale against the thresholds of the light elements and included additional data on P, K, Fe, Br, Sb, and I.

In the first three sets of data all thresholds were determined only in terms of the Cu^{63}

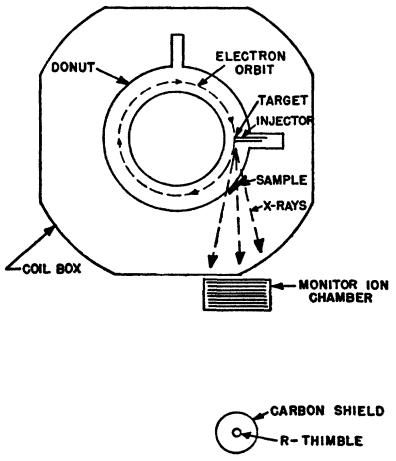

FIG. 1. Sample and monitor arrangements.

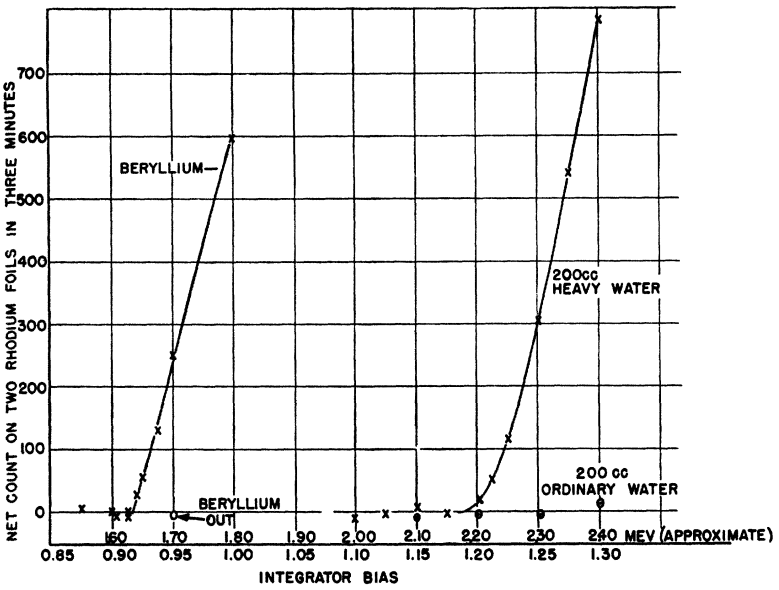

FIG. 2. Thresholds of deuterium and beryllium observed with rhodium neutron detector.

threshold as 10.9 Mev, with electrical checks on the linearity of the scale and the effective zero of the integrator bias scale. Although different trigger circuits were used at various times, it is not likely that these introduced inconsistencies which are comparable to the errors involved in estimating actual thresholds from the observed activities.

The x-ray intensity was occasionally measured by the use of a Victoreen roentgen meter. The *R*-thimble was surrounded by two inches of air-equivalent material such as carbon or hard rubber and was placed at the center of the x-ray beam at a distance of one meter from the target. The x-ray intensity measured in this manner was about 50*R* per minute at 20 Mev. In all threshold measurements it was most convenient to use the monitor chamber which was mounted on the betatron and whose output was read from a microammeter mounted on the control panel. For some of the data where it is desirable to normalize the data to the x-ray intensity in *R* per minute, the monitor readings were converted to *R* per minute by experimentally determined conversion factors.

DATA ON SPECIFIC REACTIONS

1. $H^2(\gamma, n)H^1$

The threshold for this reaction is well known and is usually given as 2.19 Mev.[3] It was observed in this case by placing 200 grams of heavy water in a bottle imbedded in paraffin near the x-ray target in the betatron. A rhodium foil was placed along one side of the heavy water container and covered with a slab of paraffin about $\frac{3}{4}$-inch thick. The samples were irradiated with x-rays at various integrator bias settings for two minutes. The rhodium foil was rolled up inside a cylinder, placed over a cylindrical Geiger counter, and the net count in the interval from $\frac{1}{2}$ to $3\frac{1}{2}$ minutes after the end of the irradiation was observed. The data are shown in Fig. 2. It is clear that the sensitivity of this method is sufficient to establish a convenient and accurate calibration point at the low energy end of the energy scale.

2. $Be^9(\gamma, n)Be^8$

This reaction has a threshold which is usually given as 1.63[3] Mev and serves the same purpose as deuterium as a check on the low end of the energy scale. The method was identical with that used for deuterium except that the heavy water was replaced with an equal mass of beryllium. The data are shown in the same figure. The threshold seems somewhat better defined than that of deuterium.

3. $Li^7(\gamma, p)He^6$ 0.8-second β^-

A cylinder of metallic lithium was irradiated at about the monitor position, and the 0.8-

[3] W. E. Stephens, Rev. Mod. Phys. **19**, 19 (1947).

second activity of He^6 was observed by means of a Geiger counter. The preliminary value of the threshold reported was obtained by placing the Geiger counter surrounded by lithium directly in the x-ray beam. The output of the counter was sent through a gating circuit so that the counts could be observed during the $\frac{3}{4}$-cycle following the x-ray burst. The results of these runs indicated a threshold of about 9.5 Mev for the short period activity. Although the sensitivity of this method is greater because of the increased counting time, it was felt that the backgrounds were less reliable than those for data taken with the counter out of the x-ray beam. The data taken by dropping the sample over a counter set up below the beam were taken a number of times, and one set of data is shown in Fig. 5. The activity seems to be definitely above background at 10.6 Mev, and the extrapolated threshold for this activity seems to lie at about 10.3 Mev. The mass data and disintegration energies give a value 10.1 Mev for the threshold,[4] but since this reaction involves the emission of protons, it is not likely that the reaction would be observed under the conditions of this experiment at energies much less than 0.5 Mev above the true threshold.

Tests were made to show that no error was made as a result of possible neutron capture in Li^7 forming the 0.88 second Li^8 activity. It is still possible that some of the observed activity may be produced by a secondary reaction in the lithium, such as $Li^6(\gamma, n)Li^5$ and $Li^6(n, p)He^6$, which would be energetically possible at about 8 Mev.

4. $C^{12}(\gamma, n)C^{11}$ 20.5-minute β^+

The threshold for this reaction was poorly defined in the earlier work[1] because of the low yield.

The substance used in the present data was thiophene-free benzene. Although this was the best of the substances tried, it still showed an appreciable background activity which is presumably due to the presence of small amounts of nitrogen or oxygen. About 50 cc of benzene was placed in a glass bottle and irradiated at various integrator settings for a period of 20 minutes. The irradiated benzene was poured into a container surrounding a Geiger counter. The data are shown in Fig. 3. The threshold can be seen to be no higher than 18.7 Mev on the scale which fixes the Cu^{63} threshold at 10.9 Mev. The threshold calculated from mass data and the disintegration energy of C^{11} is 18.7 ± 0.1 Mev.

5. $N^{14}(\gamma, n)N^{13}$ 10-minute β^+

The accuracy of the original data on this threshold was also limited by the low x-ray intensity available. It was felt that better data on this reaction might serve as an additional check on the energy scale at about the threshold of copper.

Dicyandiamide powder ($C_2H_4N_4$) was placed in a container as near to the x-ray target as possible and irradiated for periods of 30 minutes. At the end of the irradiation the powder was transferred to three cylindrical containers which fit snugly over the three Geiger counters and counted for a period of 20 minutes. A copper cylinder mounted on the monitor chamber was irradiated simultaneously, so as to obtain an accurate comparison of the two thresholds.

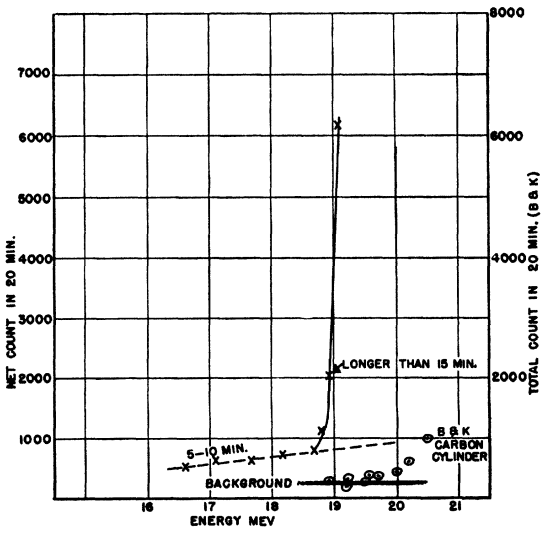

FIG. 3. Threshold of carbon as determined by activity in thiophene-free benzene. The data of Baldwin and Koch are shown on the same scale to indicate the increased activity obtained in the present experiments.

[4] The masses used in this work unless otherwise noted are those published in: H. A. Bethe, *Elementary Nuclear Theory* (John Wiley and Sons, Inc., New York, 1947).
A compilation of masses given by Mattauch will also be referred to. These are taken from J. Mattauch and S. Fluegge, *Nuclear Physics Tables and an Introduction to Nuclear Physics* (Interscience Publishers, Inc., New York, 1946).

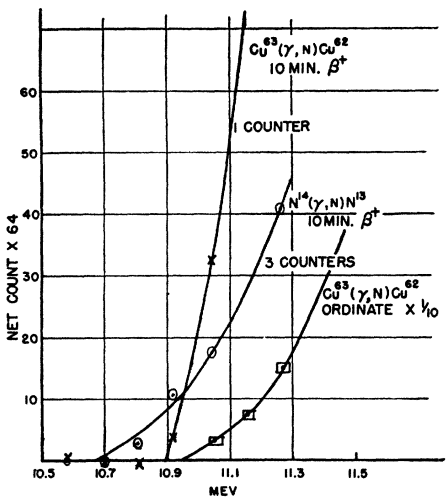

FIG. 4. Comparison of the thresholds for (γ, n) reactions in N^{14} and Cu^{63}.

The data are shown in Fig. 4. The ordinate for the nitrogen curve represents the net count from three counters in the interval of from 4 to 28 minutes after the irradiation. That for the copper curve represents the difference in the counts in the intervals from 5 to 17 and 17 to 29 minutes after the irradiation. The difference method of analyzing the copper data is desirable to eliminate possible confusion with the 12.8-hour activity which has a threshold of about 10.2 Mev.

The nitrogen activity is still too weak to define the threshold with high accuracy, but it can be seen to lie below copper by about 0.2 Mev. With higher sensitivity it is likely that the apparent threshold will be reduced somewhat. We would therefore place this threshold as 0.25 ± 0.10 Mev below that of copper. On the present scale the threshold energy would be 10.65 Mev. That calculated from the masses is 10.51 ± 0.1 Mev.

6. $Mg^{24}(\gamma, n)Mg^{23}$ 11.6-second β^+

The excitation curve near threshold was taken by the drop method and is shown with others taken by the same method in Fig. 5. The threshold from these data is estimated to be 16.2 ± 0.3 Mev, which is somewhat lower than a preliminary value of 16.5 Mev reported earlier. This value is in fair agreement with mass data which give a value of 15.5 ± 1.0 Mev.

7. $Mg^{25}(\gamma, p)Na^{24}$ 14.8-hour β^-

The experimentally determined threshold for this reaction is not expected to be well defined

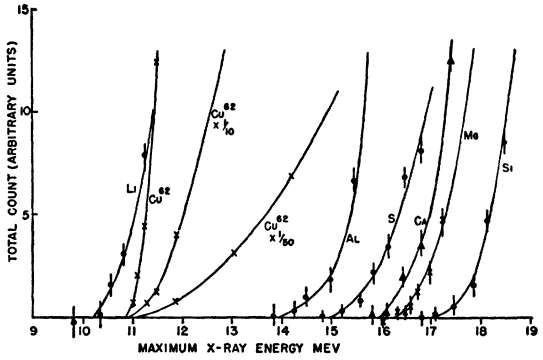

FIG. 5. Threshold for short period activities obtained by the drop method. The activation curve for Cu^{62} is sketched to various scales for comparison.

since the reaction will not occur with any probability until the energy of the protons is sufficient to penetrate a barrier of about three Mev. It was of interest, however, to compare the shape of the excitation function of this reaction with that of a (γ, n) reaction in the same element. A complete excitation curve was taken simultaneously with that of the 11.6-sec. (γ, n) activity. These data are shown in Fig. 6, and it can be seen that there is no marked difference in the shapes of the excitation functions except for the shift in the observed thresholds. The excitation curve near the threshold is shown in more detail in the inset of the same figure. The activity becomes observable at about 13 Mev. The proton binding energy calculated from the masses is 10.9 ± 1.0 Mev. When the barrier penetration is taken into account, the agreement of the observed value with the calculated value is satisfactory.

Since the 14.8-hour activity could be produced by an (n, p) reaction in Mg^{24}, it was of interest to determine whether this process contributed to the observed activity. Since the neutrons are distributed more isotropically than the x-rays, the Na^{24} activity induced as a function of the position of the sample would be different in two cases. Strips of copper and magnesium were placed across the center of the x-ray beam and irradiated. The counting rates in these two materials are shown in Fig. 7.

The angular distribution measured in this way was also useful in estimating the effective thickness of the x-ray target by comparing it with

the angular distributions calculated by Schiff.[5] One may note that the width of the x-ray beam as measured by the higher threshold reaction is somewhat less than that measured with the Cu detector.

A more sensitive way of estimating the magnitude of a possible (n, p) reaction was to irradiate a sample of phosphorus at the same position. The 170-minute Si^{31} activity indicated an excitation curve of the form shown in the inset of Fig. 6. Since the threshold for the $Mg^{24}(n, p)Na^{24}$ reaction is much higher than that for P^{31}, the strength of the (n, p) induced activity in magnesium would be several times lower than that indicated in the figure.

8. $Mg^{26}(\gamma, p)Na^{25}$ 62-second β^-

A complete excitation curve for this activity was taken simultaneously with that for Fe^{53} and is shown in Fig. 8. It can be seen to be almost identical in shape to that for Fe. The activity was observed down to values of about 15.5 Mev which would indicate that the threshold may be about 14 Mev. This is to be compared with 15.0±1.6 Mev as calculated from mass data and disintegration energies and with 14.0 Mev using the theoretically estimated mass of Na^{25}.

A chemical separation was made which indicated that the 62-second activity was due to sodium and confirmed the earlier assignment of this isotope.[6]

An absorption measurement indicated a beta-energy of 3.4 Mev. The absorption data failed to show the two groups of 2.7 and 3.7 Mev reported by Bleuler and Zunti.[7]

9. $Al^{27}(\gamma, n)Al^{26}$ 7-second β^+

The excitation curve for this reaction was obtained by the drop method and is shown in Fig. 5. The threshold can be estimated to be about 14.0±0.4 Mev. This value is somewhat lower than the preliminary value of 14.4 Mev[2], but is considerably greater than the value of 11.1±1.0 which is based on values given for the masses.

10. $Si^{28}(\gamma, n)Si^{27}$ 5-second β^+

Metallic silicon crystals were held together by a small amount of paraffin to form a thick

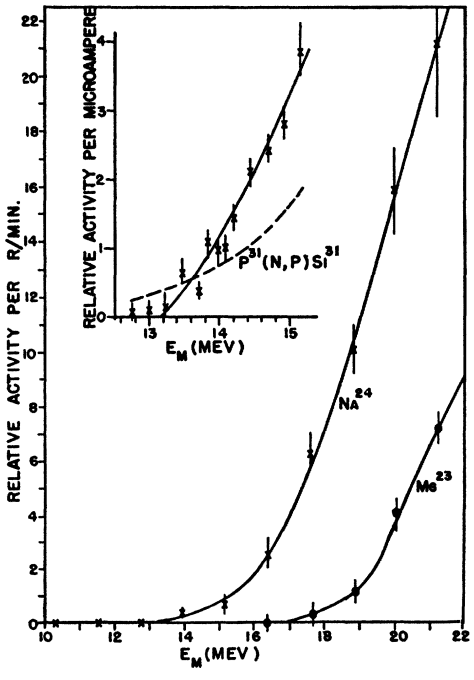

FIG. 6. Excitation curve for $Mg^{25}(\gamma, p)Na^{24}$.

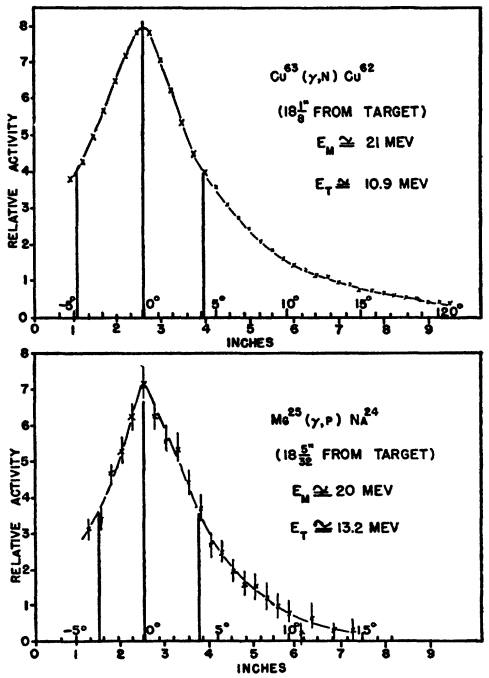

FIG. 7. Angular distribution of x-ray intensity as measured by copper and magnesium detectors.

[5] L. I. Schiff, Phys. Rev. **70**, 87 (1946).

[6] Huber, Lienhard, Scherrer, and Waffler, Helv. Phys. Acta. **16**, 33 (1943); **16**, 431 (1943); **17**, 139 (1944).

[7] E. Bleuler and W. Zunti, Helv. Phys. Acta. **20**, 199 (1947).

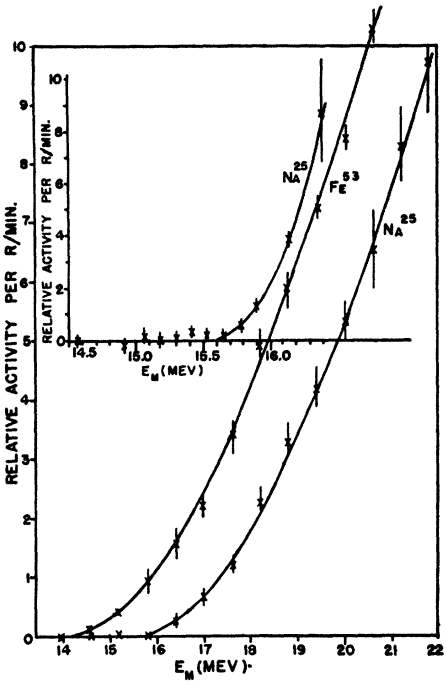

FIG. 8. A comparison of the activation curves for Na^{25} and Fe^{53}. The Na^{25} activity near threshold is shown in more detail in the inset.

cylindrical sample. The data were taken by the drop method and are shown in Fig. 5. These data indicate a threshold of about 16.8±0.4 Mev. Masses lead to a value of 16.0±1.0 Mev.

11. $P^{31}(\gamma, n)P^{30}$ 2.5-minute β^+

Red phosphorus was irradiated for periods of 4 minutes and counted for 10 minutes. The data are shown in Fig. 9. The threshold can be estimated to be about 12.35±0.2 Mev. This is again somewhat above the value of 11.1 Mev calculated from the masses given by Bethe. Mattauch's tabulation of masses, however, leads to a value of 12.2±0.5 Mev.

12. $S^{32}(\gamma, n)S^{31}$ 3.2-second β^+

Cylinders of cast sulphur were irradiated for 10 seconds and the data recorded by the drop method. The data are shown in Fig. 5, which indicates a threshold somewhat below 15.0 Mev. The value of the threshold is perhaps better stated as 14.8±0.4 Mev. The masses given by Bethe and by Mattauch again differ appreciably, leading to values of 16.7±0.5 and 14.9±0.5 Mev, respectively. The half-life was found to be 2.6 ±0.2 seconds, which is considerably lower than that usually given.

13. $K^{39}(\gamma, n)K^{38}$ 7.5-minute β^+

Potassium carbonate (K_2CO_3) powder was irradiated for 10-minute intervals and counted for periods of 18 minutes. The natural radioactivity of K^{40} gave rise to a rather large background. The threshold, as shown in Fig. 10, seemed fairly well defined as about 13.2±0.2 Mev. Masses are known very inaccurately. Those given lead to a value of 12.7±1.5 Mev.

14. $Ca^{40}(\gamma, n)Ca^{39}$ 1-second β^+

Samples of calcium fluoride (CaF_2) crystals were made up into a cylinder by a small amount of paraffin binder and irradiated for periods of two seconds. The data were obtained by the drop method. The short period made it difficult to obtain good accuracy, but the records showed definite indications of the short period at energies above 16.3 Mev. The resulting threshold is perhaps best stated as 15.9±0.4 Mev. The masses are again only approximately known. These lead to a value of 13.7±1.5 Mev.

15. $Fe^{54}(\gamma, n)Fe^{53}$ 8.9-minute β^+

The threshold for this activity was observed by Baldwin and Koch to be below 14.2 Mev. The present data were taken with pure electrolytic iron foil irradiated as close to the x-ray target as possible. The threshold was estimated to lie at about 13.8±0.2 Mev on the present

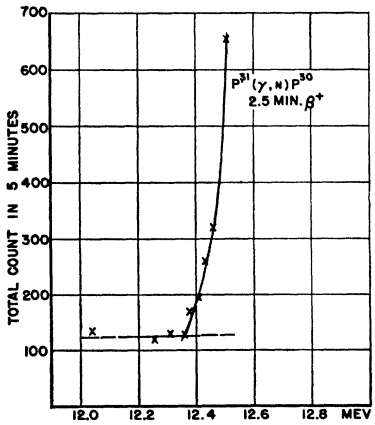

FIG. 9. Threshold curve for the $P^{31}(\gamma,n)P^{30}$ reaction.

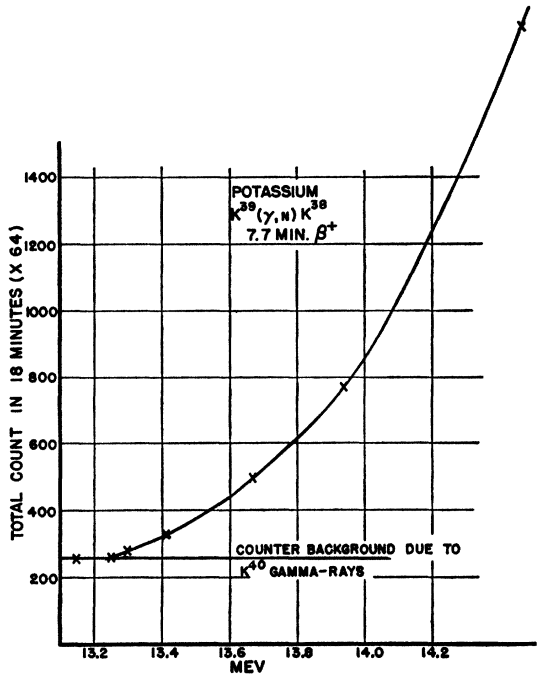

FIG. 10. Threshold curve for $K^{39}(\gamma, n)K^{38}$ reaction.

energy scale. A complete excitation curve for this activity taken simultaneously with that of $Mg^{26}(\gamma, p)Na^{25}$ is shown in Fig. 8.

16. $Cu^{65}(\gamma, n)Cu^{64}$ 12.8-hour $\beta^+\beta^-$

Copper samples $3\times2\times0.005$ inches were folded up, covered with cadmium and taped on to the donut so as to intercept the maximum x-ray flux. These were wrapped around a Geiger counter, and the activity was followed for about one half-life. The data are shown in Fig. 11. The shaded area represents the average neutron-induced activity in the sample, which to some extent limits the accuracy. The threshold for this activity can perhaps be best represented by a value of 10.2 ± 0.2 Mev.

A complete excitation curve for this activity was taken simultaneously with that for Cu^{63} which is shown in the same figure. The two curves are similar except for the energy shift. The errors attached to the Cu^{64} points are largely due to the interpretation of the x-ray intensity measurements, which were complicated by the close irradiation geometry. Since the activities were observed in the same copper sample the errors in the relative activities are much less.

17. $Cu^{63}(\gamma, n)Cu^{62}$ 10-minute β^+

Copper cylinders with $\frac{1}{16}$-inch walls, 4 inches long, and $\frac{3}{4}$ inch in diameter were placed in a cadmium holder on the monitor chamber and irradiated for periods of about five minutes and counted for about five minutes. This threshold was observed about thirty times during this work. The integrator bias setting for this threshold was found to be reproducible to better than 0.2 percent and was used as a calibration point on the energy scale at 10.9 Mev.

18. $Br^{79}(\gamma, n)Br^{78}$ 6.4-minute β^+

Samples of NaBr powder were irradiated for 10 minutes, transferred to a 1×2-inch lead tray (T), and placed between the poles of a small magnetron magnet as shown in Fig. 12. The simple magnetic separation made it possible to detect this positron activity above the large background resulting from the 18-minute beta-activity formed from Br^{81}. The counting rate in this case is only about 1 percent of that for the 18-minute activity but the threshold is still fairly well defined. It is definitely below 10.8

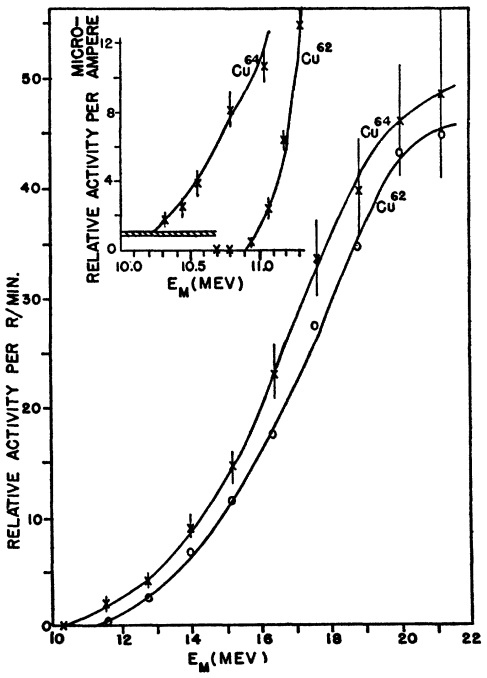

FIG. 11. Excitation curves for Cu^{64} and Cu^{62} taken simultaneously. The curves near threshold are shown in more detail in the inset.

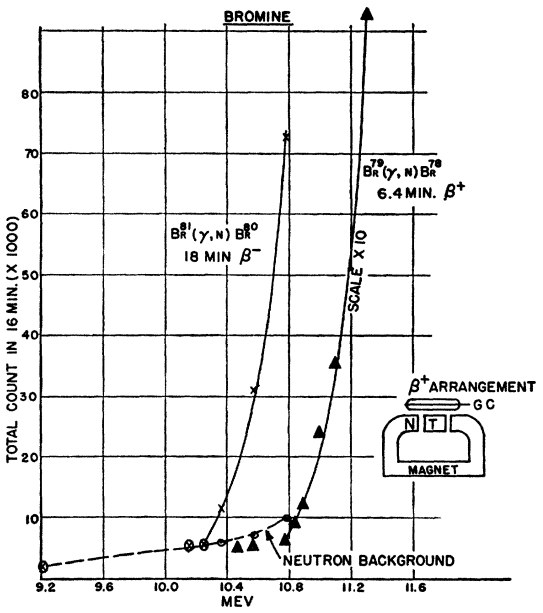

FIG. 12. Thresholds for induced activities in bromine.

Mev and is perhaps better expressed as 10.7 $\pm$0.2 Mev.

19. $Br^{81}(\gamma, n)Br^{80}$ 18-minute β^-

The NaBr powder was irradiated for periods of 15 minutes and counted in a cylindrical powder holder surrounding a Geiger counter. The background caused by neutron capture in Br^{79} was determined simultaneously by placing an additional sample of NaBr outside the x-ray beam and normalizing at a point well below the (γ, n) threshold. The threshold may be stated as 10.2$\pm$0.2 Mev.

20. $Sb^{121}(\gamma, n)Sb^{120}$ 17-minute β^+

Antimony powder was irradiated for 15 minutes and transferred to a powder holder surrounding a Geiger counter. The activity had a clean 17-minute half-life. The total count in 20 minutes at various energies is shown in Fig. 13. The threshold can be seen to lie at about 9.25 $\pm$0.2 Mev.

21. $I^{127}(\gamma, n)I^{126}$ 13-day β^- K

The long life of the induced activity in this case makes it impractical to obtain the threshold by observing the induced activity, and an attempt was made to observe the accompanying neutrons. These neutrons must, however, be detected above the normal background of neutrons from the betatron itself.

Five pounds of crystalline iodine were placed in a glass jar with a one-inch aluminum tube through the center. This jar was surrounded by paraffin and placed in the x-ray beam. One rhodium foil was placed in a polystyrene holder inside the iodine bottle while a similar rhodium foil was placed outside the x-ray beam near the "donut." The data are shown in Fig. 14. The threshold is most clearly displayed by the ratio of the activities in the two foils and seems to lie at about 9.3$\pm$0.2 Mev.

22. $Ta^{181}(\gamma, n)Ta^{180}$ 8.2-hour β^- K

Tantalum metal foil was taped on to the donut and irradiated for one hour. It was then formed into cylinders and counted for at least one half-life. The activity had a clean 8.2-hour half period. The 14-minute activity reported by Bothe and Gentner was not observed.[8] This activity may have been that of the 16-minute isomer of Ta^{182} reported by Seren, Friedlander, and Turkel,[9] which was too weak to be observable under the conditions of this experiment.

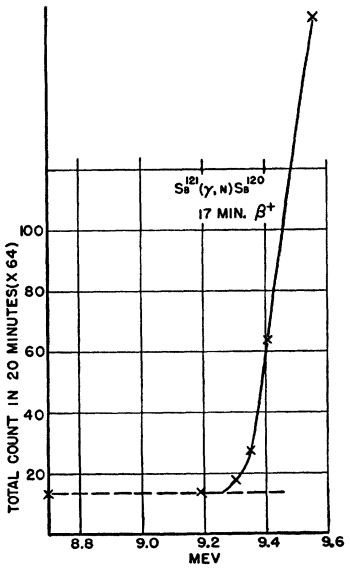

FIG. 13. Threshold for $Sb^{121}(\gamma, n)Sb^{120}$.

[8] W. Bothe and W. Gentner, Zeits. f. Physik. **105**, 236 (1937).
[9] L. Seren, H. N. Friedlander, and S. Turkel, Phys. Rev. **72**, 163 (1947).

The data on the excitation function for the 8.2-hour period are shown in Fig. 15. The threshold seems to lie below 7.8 Mev and may be stated as 7.7 ± 0.2 Mev.

A complete excitation curve taken simultaneously with that of copper is shown in the same figure. This excitation curve shows an abrupt change of slope at about 18 Mev which indicates a drop in the cross section for the formation of this activity at this energy. This feature of the curve is not characteristic of the monitor used since the copper was subject to the identical irradiation in each case and does not show a break at this point. Baldwin and Klaiber have shown that there is a similar break in the copper excitation curve at about 24 Mev. Cross sections based on the theoretical x-ray spectrum can be estimated only roughly. Those calculated by an empirical treatment of the data similar to that used by Baldwin and Klaiber[10] give the cross sections indicated in Fig. 16. The absolute cross section for tantalum may be larger than that indicated in the figure, since the decay scheme of Ta^{180} is not certain. It should be emphasized that, although the cross sections are consistent with our data and the theoretical spectrum, the nature of the data makes them relatively insensitive to the detailed shape of the cross sections. At higher energies a point by point analysis of the data indicated that the errors in the cross sections were much greater than the individual values represented by the curves in the figure.

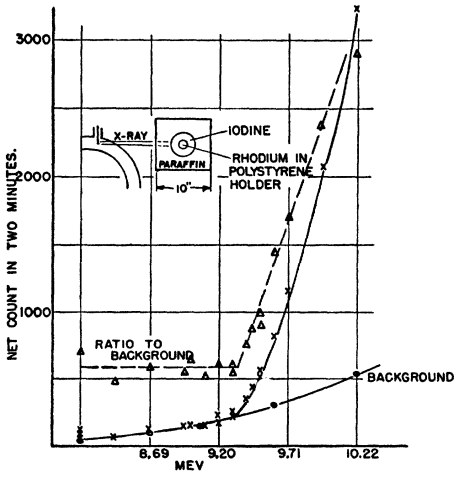

FIG. 14. Threshold for production of neutrons from iodine.

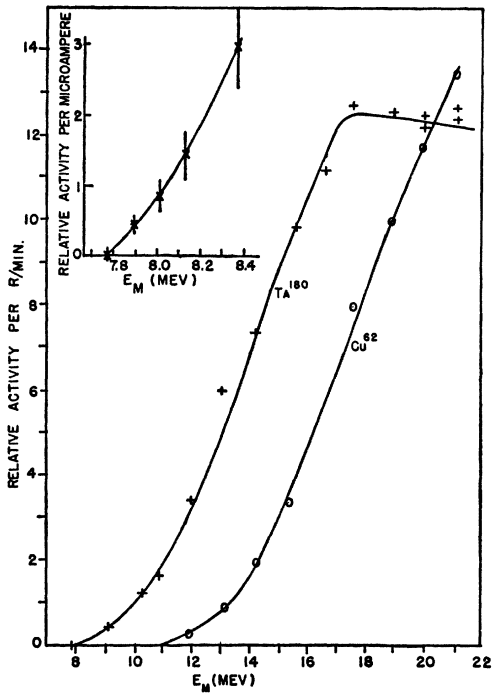

FIG. 15. Excitation curve for tantalum taken simultaneously with that for copper.

23. $Bi^{209}(\gamma, n)Bi^{208}$

A number of attempts failed to detect any radioactivity from this reaction. There has been some evidence which indicates the existence of a long life electron emission.[11]

The threshold for this reaction was determined by detecting the neutrons from an arrangement similar to that used for beryllium and deuterium. The intensity of neutrons from the betatron is still fairly low at these energies, so that the threshold can be distinguished from the rising background. The data are shown in Fig. 17. The threshold is estimated from the data to be 7.45 ± 0.2 Mev. The first measurement, which was taken with less satisfactory energy calibrations, gave a value of 7.3 Mev. It can be seen that the neutron background becomes significant at about 6.5 Mev. This energy is about that expected for the threshold for the most loosely bound neutron in the platinum x-ray

[10] G. C. Baldwin and G. S. Klaiber, Phys. Rev. **73**, 1156 (1948).

[11] J. J. Howland, D. H. Templeton, and I. Perlman, Phys. Rev. **71**, 552 (1947).

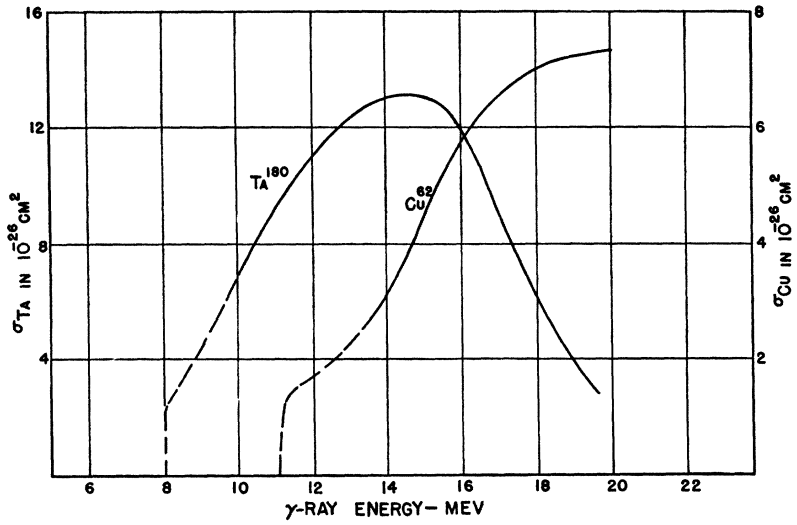

FIG. 16. Approximate cross sections for tantalum and copper as estimated from the excitation curves. The broken lines near the threshold are those obtained by estimating the effect of target thickness on the shape of the x-ray spectrum. The solid line portion of the curves are those calculated by using the theoretical spectrum as a function of energy and are approximately proportional to the derivative of product of E and excitation curves shown in Fig. 15.

target. A comparison of the number of neutrons from the betatron with that from a Ra-Be photoneutron source indicated that the total neutron yield from the betatron was about 5×10^8 neutrons per second at 20 Mev.[12] The number drops to about 10^5 neutrons per second at about 7 Mev. The general trend of the neutron-induced activities at higher energies is indicated by the background curve on the reduced scale.

DISCUSSION

Excitation Curves

It is found that the excitation curves near the threshold for all the reactions observed were very similar in shape and could be represented by a function $Y=kx^2$, where Y is the yield per unit of x-ray intensity measured by the ionization in a thick-walled ionization chamber, and x is the difference between the maximum x-ray energy and the observed threshold energy. This relation seemed to hold for a region of about 3 Mev. Since the effective thickness of the x-ray target is about 1.5 Mev, as estimated from the angular spread of the x-rays, the intensity of any isochromat in the x-ray spectrum in the region of maximum x-ray energy may be expected to increase with the energy below the maximum. If one assumes such a spectrum, the quadratic excitation functions observed would indicate that the cross sections rise abruptly to reasonably large values at a fraction of a Mev above threshold. This is in agreement with the results of Bothe and Gentner[13] which indicated that the cross section for Cu^{63} was about 2×10^{-26} and 5×10^{-26} cm^2 at 12 and 17 Mev, respectively.

The cross section for production of 10-minute copper activity averaged over the useful part of the x-ray spectrum at 20 Mev was estimated from ionization chamber measurements by the method discussed by Strieb, Fowler, and Lauritsen[14] and was found to be about 4×10^{-26} cm^2. This is in good agreement with Bothe and Gentner's values, but lower than that of other recent measurements.[15] The abrupt reduction of the cross sections at higher energies has not been satisfactorily explained. The small cross sections observed for the competing reactions[16] would seem to indicate that the explanation is a more subtle one than that of competition with other reactions which become possible at the higher energies.

The applicability of the Breit-Wigner dispersion formula to photo-nuclear reactions has been discussed in a number of papers.[17] Kalckar,

[12] We are indebted to M. Goldhaber for the loan of the calibrated neutron source.

[13] W. Bothe and W. Gentner, Zeits. f. Physik. **112**, 45 (1939).

[14] J. F. Streib, W. A. Fowler, and C. C. Lauritsen, Phys. Rev. **59**, 215 (1941); W. A. Fowler, C. C. Lauritsen, and T. Lauritsen, Rev. Mod. Phys. **20**, 236 (1948).

[15] H. Waffler and O. Hirzel, Helv. Phys. Acta **21**, 200 (1948); Skaggs, Laughlin, Hanson, and Orlin, Phys. Rev. **73**, 420 (1948).

[16] M. L. Perlman and G. Friedlander, Phys. Rev. **74**, 442 (1948).

[17] H. A. Bethe and G. Placzek, Phys. Rev. **51**, 450 (1937); F. Kalckar, J. R. Oppenheimer, and R. Serber,

Oppenheimer, and Serber reached the conclusion that the cross sections for the heavier elements should reach a maximum at energies where the level widths are of the same order as the level spacings and would decrease with further increases in the gamma-ray energies. It does not seem likely, however, that this treatment would explain the reductions in cross sections which are suggested by the data of Baldwin and Klaiber as well as by the present data for tantalum. Recently Goldhaber and Teller have suggested that the excitation curves could be accounted for by assuming a special type of resonance absorption in which the protons move in unison with respect to the remainder of the nucleus.[18]

Correlation of Threshold Data with Packing Fraction Curve

The experimental determinations of (γ, n) thresholds for light elements serve to check the energy scale, and, for masses above 20, serve to establish mass differences with somewhat greater accuracy than has been done previously. The observed thresholds and the binding energies obtained from the masses are summarized in Table I.

The masses above 40 are in most cases so poorly known that neutron binding energies can not be calculated directly with any accuracy. It is of interest, however, to correlate the observed binding energies with those calculated from the packing fraction by the method outlined by Bohr and Wheeler.[19] It has been found that the experimental data can be used to establish an approximate empirical relation to express the masses as a function of the atomic and mass numbers Z, and A.[20]

$$M(A,Z)=A-0.0081\cdot Z-0.00611\cdot A+0.014\cdot A^{\frac{2}{3}}+0.083[(A/2-Z)^2/A]+0.000627Z^2/A^{\frac{4}{3}}+\delta, \quad (2)$$

TABLE I. Observed thresholds.

Reaction	Observed activity	Observed thresholds (Mev)	Thresholds calculated from masses (Mev)
$H^2(\gamma, n)H^1$	Neutrons	2.20±0.05	2.19±0.03
$Be^9(\gamma, n)Be^8$	Neutrons	Calibration	1.63±0.03
$Li^7(\gamma, p)He^6$	0.85 β^-	9.8±0.5[a]	10.1 ±0.5
$C^{12}(\gamma, n)C^{11}$	20.5-min. β^+	Calibration	18.7 ±0.1
$N^{14}(\gamma, n)N^{13}$	10-min. β^+	10.65±0.2	10.51±0.1
$Mg^{24}(\gamma, n)Mg^{23}$	11.6-sec. β^+	16.2±0.3	15.5±1.0
$Mg^{25}(\gamma, p)Na^{24}$	14.8-hr. β^-	11.5±1.0[a]	10.9±1.0
$Mg^{26}(\gamma, p)Na^{25}$	62-sec. β^-	14.0±1.0[a]	15.0±1.6
$Al^{27}(\gamma, n)Al^{26}$	7-sec. β^+	14.0±0.4	11.1±1.0
$Si^{28}(\gamma, n)Si^{27}$	5-sec. β^+	16.8±0.4	16.0±1.0
$P^{31}(\gamma, n)P^{30}$	2.5-min. β^+	12.35±0.2	11.1±1.0
$S^{32}(\gamma, n)S^{31}$	3.2-sec. β^+	14.8±0.4	16.7±0.5
$K^{39}(\gamma, n)K^{38}$	7.5-min. β^+	13.2±0.2	12.7±1.5
$Ca^{40}(\gamma, n)Ca^{39}$	1-sec. β^+	15.9±0.4	13.7±1.5
$Fe^{54}(\gamma, n)Fe^{53}$	8.9-min. β^+	13.8±0.2	
$Cu^{65}(\gamma, n)Cu^{64}$	12.8-hr. $\beta^+\beta^-$	10.2±0.2	
$Cu^{63}(\gamma, n)Cu^{62}$	10-min. β^+	10.9±0.2	
$Br^{79}(\gamma, n)Br^{78}$	6.4-min. β^+	10.7±0.2	
$Br^{81}(\gamma, n)Br^{80}$	18-min. β^-	10.2±0.2	
$Sb^{121}(\gamma, n)Sb^{120}$	17-min. β^+	9.25±0.2	
$I^{127}(\gamma, n)I^{126}$	Neutrons	9.3±0.2	
$Ta^{181}(\gamma, n)Ta^{180}$	8.2-hr. β^-	7.7±0.2	
$Bi^{209}(\gamma, n)Bi^{208}$	Neutrons	7.45±0.2	

[a] These values are reduced from experimentally observed thresholds by approximately one-half the height of the barrier for proton emission.

where δ is zero for odd A, $-0.036/A^{\frac{1}{2}}$ for even A odd Z, and $+0.036/A^{\frac{1}{2}}$ for even A even Z. The neutron binding energy of a neutron in a nucleus of mass number A and atomic number Z is then

$$E_b(A,Z)=M(A-1,Z)+M_n-M(A,Z)\cong 83(Z^2/A^2)[1+0.0025A^{\frac{2}{3}}]-9.33/A^{\frac{1}{3}}-5.72+36/A^{\frac{4}{3}} \text{ millimass units.} \quad (3)$$

The positive value of δ used in this case holds for odd A odd Z, and even A even Z nuclei, which includes all nuclei observed in the present work.

Feenberg has attempted to evaluate the empirical relations in more detail and to take into

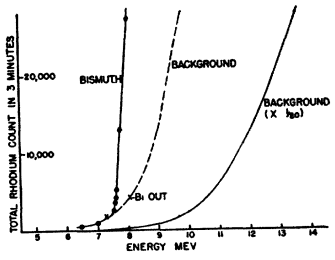

FIG. 17. Excitation curve for neutrons from bismuth. A more extensive curve indicating the effective background of neutrons from the betatron is shown on a reduced scale to higher energies.

Phys. Rev. **52**, 273 (1937); N. Bohr, R. Peierls, and G. Placzek, Nature **144**, 200 (1939); V. F. Weisskopf and D. H. Ewing, Phys. Rev. **57**, 472, Eq. (12) (1940), L. I. Shiff, Phys. Rev. **73**, 1311 (1948).

[18] M. Goldhaber and E. Teller, Phys. Rev. **74**, 1046 (1948).

[19] N. Bohr and J. H. Wheeler, Phys. Rev. **56**, 428 (1939); H. A. Bethe and R. F. Bacher, Rev. Mod. Phys. **8**, 82 (1936); C. F. Weizsacher, Zeits. f. Physik. **96**, 431 (1935); K. Way and E. P. Wigner, Phys. Rev. **73**, 1318 (1948).

[20] M. G. Mayer, Phys. Rev. **74**, 235 (1948); Mattauch and Flugge (reference 4, p. 100) give a similar equation.

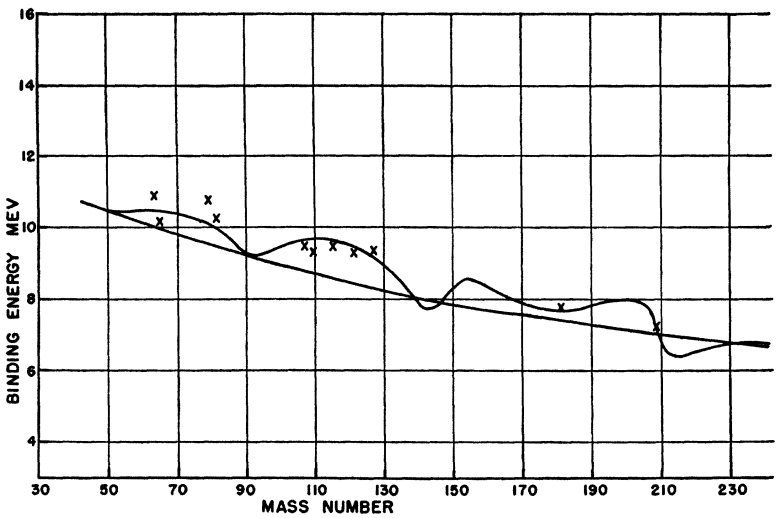

FIG. 18. Observed thresholds for (γ, n) reactions in odd nuclei. The solid lines represent the binding energy for odd A nuclei which lie at the bottom of the mass valley. The smooth curve is that calculated by use of Eq. (3). The irregular curve is based on Feenberg's curve for the mean excitation energy produced by the capture of a slow neutron.

account the fact that Z, for nuclei along the mass valley, is not a smooth function of the mass as assumed above.[21] He has calculated average neutron binding energies as a function of A. These are displayed in Fig. 4 of his paper. The binding energies for individual isotopes can be determined from Eq. (62) and the data shown in Figs. 3, 4, and 5 and Table 6 of the same paper. The binding energy for odd A odd Z and even A even Z nuclei which lie along the mass valley are shown by the irregular curve in Fig. 18. The additional binding energies for these types of nuclei which lie off the center of the valley are given approximately by the expression

$$\Delta E = 74/A[Z - Z_{(A-\frac{1}{2})}] \text{ Mev}, \qquad (4)$$

where $Z_{(A-\frac{1}{2})}$ is the value of Z corresponding to the most stable hypothetical nucleus having a mass of $(A-\frac{1}{2})$.

TABLE II. Observed and calculated thresholds.

Element	A	Z	Z_A	Binding energy Eq. 3	Binding energy Feenberg	Observed thresholds
Fe	54	26	24.5	12.6	12.6	13.8±0.2
Cu	63	29	28.5	11.1	11.1	10.9 cal.
Cu	65	29	29.3	10.0	10.0	10.2±0.2
Zn	64	30	28.9	11.7	11.9	11.6±0.4*
Se	82	34	36.0	8.0	8.3	9.8±0.5*
Br	79	35	34.8	10.0	10.8	10.7±0.2
Br	81	35	35.7	9.0	9.8	10.2±0.2
Mo	94	42	41.0	10.8	10.5	13.5±0.4*
Ag	107	47	46.7	9.6	10.1	9.5±0.5*
Ag	109	47	47.5	9.0	9.4	9.3±0.5*
In	115	49	49.5	8.7	9.4	9.5±0.5*
Sb	121	51	51.0	8.4	9.6	9.25±0.2
I	127	53	53.0	8.2	9.3	9.3±0.2
Ta	181	73	73.0	7.7	7.7	7.7±0.2
Bi	209	83	83.0	7.1	7.2	7.45±0.2

* Thresholds reported by Baldwin and Koch (see reference 1).

[21] E. Feenberg, Rev. Mod. Phys. **19**, 239 (1947).

A comparison of the observed and calculated thresholds is given in Table II. This table includes all the observed thresholds reported for elements having atomic masses above 50. The odd A nuclei should have thresholds close to those calculated for elements lying along the mass valley. The agreement of the odd A thresholds with Feenberg's curve is good. It would be of interest to study the binding energies of other odd and even nuclei having A's of about 90, 140, and 210 to see if the strong variations in binding energy are confined to particular nuclei as suggested by Mayer[20] or if they can be fitted by more general fluctuations of binding energies as assumed by Feenberg.

The authors are indebted to R. T. Anderson and D. Riesen for assistance with these experiments and to H. Palevsky for the development and testing of the integrator circuits.

This work was assisted by the joint program of the Office of Naval Research and Atomic Energy Commission.

One of us (JM) wishes to acknowledge a National Research Council Fellowship held throughout much of this work.